energy incident on the nonlinear crystal was 1 mJ in 9 ns long pulses. The beam quality was approximately $M^2 = 2$ horizontally and better than 1.1 vertically. The spectral width of the pump laser has been measured to 28 GHz FWHM [11], with 1.2 GHz longitudinal mode separation corresponding to an optical cavity path length of 124 mm. An optical isolator at the output of the laser ensures that back-reflection from the OPO causes no changes in the laser output.

After passing through the isolator, a power regulating half-wave plate and polarizer the laser beam was focused to a 0.3×0.24 mm^2 waist (exp(−2) intensity radius). At the focus a 20 mm long PPKTP crystal with a 38.85 μm domain grating over 16 mm of the length was placed [14]. The crystal was heated to 57 °C to provide optimum gain near degeneracy. The crystal optical surfaces were slightly wedged and AR-coated to avoid monolithic OPO action. The crystal was surrounded by a cavity consisting of a flat dichroic incoupling mirror and a VBG, see Fig. 1. The VBG had nominally 50% peak reflectivity with 0.5 nm FWHM spectral width at 2122 nm. The theoretical power reflectivity at the idler wavelength from the VBG is less than 10^{-4}. The surfaces were AR-coated and tilted with respect to the grating vector to avoid broadband feedback. Since no surfaces other than the incoupling mirror are aligned perpendicular to the pump direction this cavity can be seen as singly resonant. This was verified by Fabry-Perot measurements of the OPO signal and idler spectra, which revealed a clear longitudinal mode structure in the signal and an unstructured idler [11]. As a reference measurement using a DRO, the VBG was replaced by a flat broadband 50% reflecting mirror covering the signal and idler bands. The positions of the incoupling mirror and PPKTP crystal were fixed while the output coupler (VBG or dielectric mirror) was translated and in each position the average OPO output energy of 100 pulses was recorded. The output spectrum with the VBG output coupler consists of two narrow spectral peaks, the signal at 2122 nm and the corresponding idler at 2135 nm. At short cavity lengths the bandwidths have been measured to 10 and 20 GHz (FWHM) for the signal and the idler, respectively [11]. In addition to the main signal and idler peaks additional wavelengths seeded by four wave mixing (FWM) are generated. The FWM is a cascaded $\chi^{(2)}$ interaction caused by second harmonic generation of the pump and idler and subsequent difference frequency generation [12,13]. Because of the wide phase matching bandwidth this parasitic interaction can reach macroscopic efficiency. In the DRO the output spectrum covers the whole range from 2020 to 2250 nm.

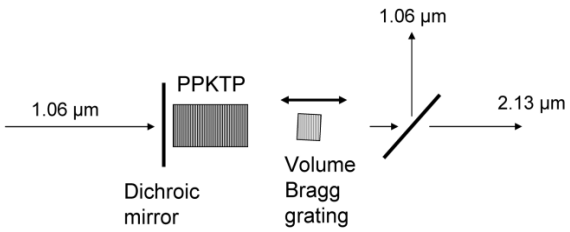

Fig. 1. The experimental setup.

3. Experimental results

The OPO output energies from the SRO for varying cavity optical path lengths and several different pump energies are shown in Fig. 2. There is approximately a factor of two difference in pump energy between the highest and lowest pump energies used with the VBG output coupler. The general trend is that the output energy is reduced as the cavity length increases. This is the typical dependence for OPOs with plane mirror cavities and is caused by increased OPO pulse development time and increased diffraction losses. The output energy shows distinct resonances with increased energy when the OPO cavity length is equal to or an integer fraction of the laser cavity length. Looking at the resonances at relatively short cavity lengths,

#126746 - $15.00USD Received 13 Apr 2010; revised 5 May 2010; accepted 5 May 2010; published 7 May 2010

where we operate up to twice the threshold and the OPO reaches the threshold off resonance for several pump energies, it is evident that the resonance strength decreases with increasing pump energy. The strength of the resonances also decreases with increasing denominator of the fractions, but close to threshold peaks for denominators up to 12 (e.g. at cavity length ratio 5/12 = 0.417) are evident.

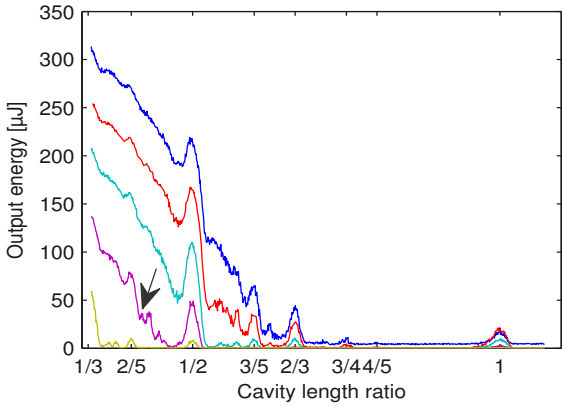

Fig. 2. Average OPO pulse energy as a function of cavity length ratio from SRO with VBG output coupler. The pump energies were 0.99, 0.93, 0.82, 0.67 and 0.50 mJ. The arrow points at the peak for cavity length ratio 5/12.

Measurements of the same variation for a broadband DRO using a dielectric mirror output coupler are shown in Fig. 3. These resonances are the same kind of resonances that are described in [1]. Although the same fractional resonances are observed for the DRO and SRO, as expected, the character of the resonances is different in the two cases. The resonance peaks in the DRO do not seem to decrease in magnitude with increasing pump power. The sharper peaks in the DRO compared to the SRO is a result of the wider bandwidth and hence shorter coherence length.

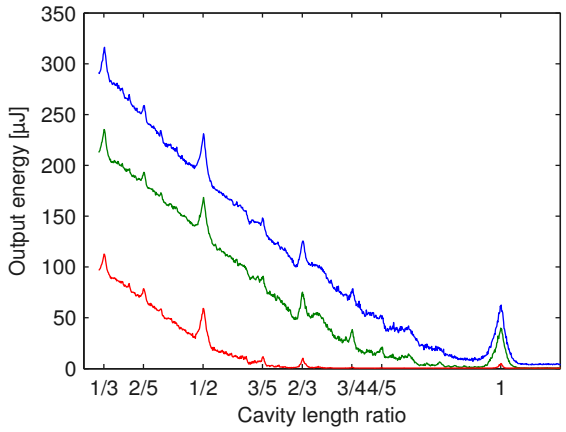

Fig. 3. Average OPO pulse energy as a function of cavity length ratio from DRO with mirror output coupler. The pump pulse energies were 0.99, 0.93 and 0.73 mJ.

The slope is steeper for the singly resonant VBG cavity than with the mirror output coupler. This is attributed to the fact that the VBG is more sensitive to incidence angle deviation and that the increased divergence of the beam in a longer cavity can reduce the effective reflectivity of the VBG [15]. The higher degree of outcoupling from the singly-resonant OPO with the VBG may also contribute.

#126746 - $15.00 USD Received 13 Apr 2010; revised 5 May 2010; accepted 5 May 2010; published 7 May 2010

To make the difference between the SRO and DRO more evident a baseline was subtracted by fitting a third order polynomial to the output energy in points that are not close to any resonance, see Fig. 4. Notice the dips in output energy surrounding the cavity length ratio ½ resonance peak that are present only in the singly resonant case, showing that different physical processes are important for SROs and DROs. Another difference is that for the SRO the peak at 3/5 is much larger than at 2/5, while they for the DRO have equal magnitude. This difference further illustrates that for the SRO the resonances decrease when the OPO operates high above threshold, while for the DRO the magnitude of the resonances remain constant.

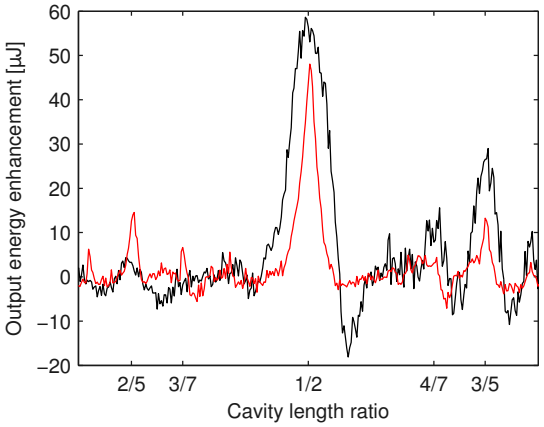

Fig. 4. Enhancement peak with general slope subtracted for a cavity length of the OPO around ½ of the laser cavity length. The black curve is the SRO with the VBG and the red curve is the DRO with the mirror output coupler, in both cases with 0.99 mJ pump energy.

4. Simulations

In order to elucidate the experimental observations we performed simulations of a SRO with a VBG output coupler using the simulation program Sisyfos, developed at FFI in Norway. The physical model behind Sisyfos is explained in [16,17], and a more complete documentation is under preparation [18]. The simulations were performed in a plane wave approximation, using only a single on axis sample in the transversal direction and neglecting diffraction, to obtain reasonable computation time. Spectral resolution and bandwidth is realized by using dense temporal sampling during the complete pump pulse. Fourier transformation of the time domain signals provides the spectrum around the carrier frequencies at the pump center frequency and at the degenerate OPO frequency. The second order nonlinear interaction is solved numerically for each step through the crystal and effects of group velocity dispersion between pump, signal and idler are included. To check that the VBG group delay dispersion was not important for the phenomenon simulations were also performed with an unphysical narrow bandwidth reflectivity mirror. No qualitative differences from the VBG case were found.

The output energy for varying cavity lengths and pump energies is shown in Fig. 5. For each point 10 plane wave simulation runs were performed and the energy averaged. The model of the pump assumes non-correlated modes where the phases and relative amplitudes are constant during the pulse. The plane wave approximation neglects diffraction losses. This clearly reduces the threshold, especially at longer cavity lengths and explains the lower slope with cavity length as compared to the experimental data. Apart from this limitation the results are in good qualitative agreement with our experimental data. The resonance peaks and the surrounding dips are confirmed in the simulations. The simulations reveal that the amplitudes of the resonances are indeed decreasing with the pump power above threshold. The reduction of the enhancement peak amplitude for increasing pump energy seems somewhat faster in the simulation than in the experiments. In the simulation the peak at cavity length ratio ½ has

#126746 - $15.00 USD Received 13 Apr 2010; revised 5 May 2010; accepted 5 May 2010; published 7 May 2010

disappeared almost completely already for twice the threshold value. In Fig. 2 the peak is on the other hand clearly visible for the highest pump energy. The persistence of the enhancement peak higher above threshold could be caused by stronger amplitude modulation in the pump laser than in the simulation model. Strong amplitude modulation associated with imperfect mode-locking can be caused by partial coherence between the longitudinal modes in the laser, which has been observed in Nd:YVO_4-lasers [19]. The phase-sensitive character of the resonances is manifested by the dips surrounding the resonant peaks.

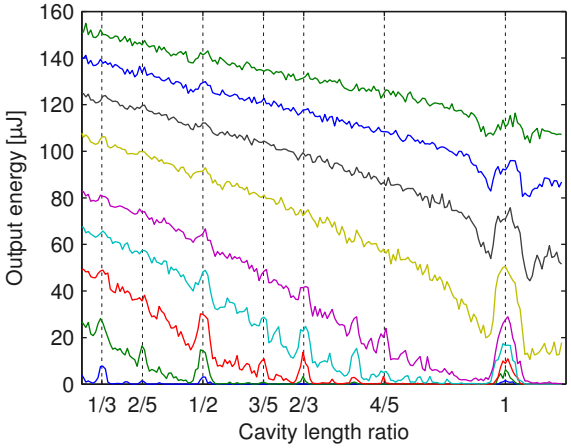

Fig. 5. Simulated output energy from SRO with VBG output coupler in plane wave simulation. The pump energies are from the bottom 100, 125, 150, 175, 200, 250, 300, 350 and 400 μJ.

5. Discussion and conclusions

The origin of the SRO cavity length resonances can easiest be understood by looking into the SRO operating close to the threshold. In the non-depleted pump approximation the signal gain after one pass through the crystal will follow that of the pump intensity variation. In a multimode pump laser the intensity will be quasi-periodic in time with a period τ corresponding to the roundtrip time in the pump laser cavity. After one roundtrip in the cavity this signal will interact with the pump radiation generated at a later time. The parametric amplification process on a single pass through the crystal can be seen as a cross-correlation between pump and signal. The cross-correlation will be higher and thus the SRO threshold will be reached faster if the roundtrip time of the OPO cavity matches the pump laser periodicity to within the width of the cross-correlation peak. This width is determined by the bandwidths of the pump and the signal. If the signal bandwidth because of cavity restrictions, is narrower than the pump bandwidth, as in our case, this can be seen as a low pass filtering of the intensity fluctuations. Signal-pump temporal walk-off caused by different group velocities in the nonlinear crystal will also constitute a low pass filter. In Fig. 6 the left pane illustrates the simulated pump and signal pulses, with the power averaged over the roundtrip time. The upper right and lower right panes in Fig. 6 show the periodic variation of the instantaneous power of the pump and the signal, respectively, over a couple of cavity roundtrip times t. It can be seen that the signal is mainly generated for time instances where the signal co-propagates with spikes in the pump power. The selected time period can from the left pane be seen to have decreasing roundtrip averaged pump power while the signal power is still increasing, as evidenced by more “micro-pulses” appearing at times in the roundtrip that correspond to lower amplitude pump spikes.

#126746 - $15.00 USD Received 13 Apr 2010; revised 5 May 2010; accepted 5 May 2010; published 7 May 2010

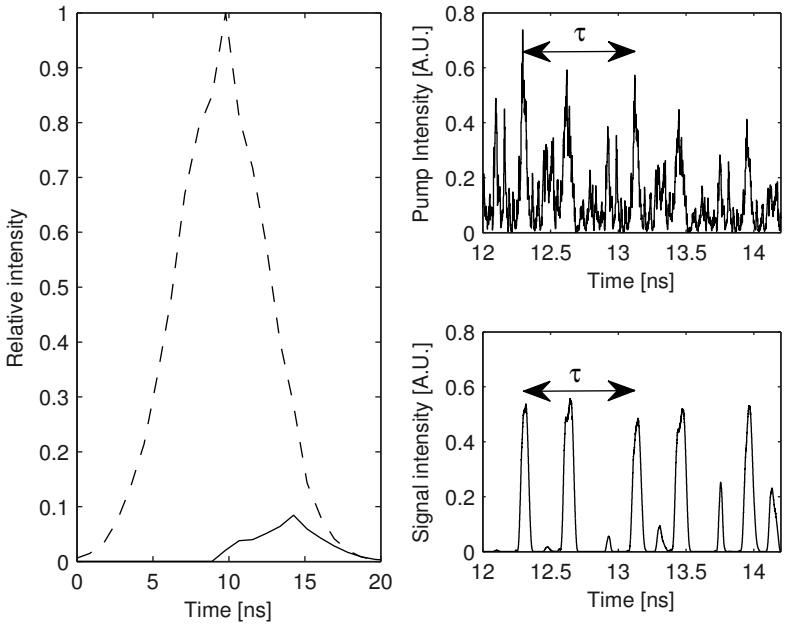

Fig. 6. Results of a simulation with equal mode separations for pump laser and OPO showing the power after the input coupler. The simulation was done with 6 GHz pump bandwidth to make pump intensity variations slower. (Left) Roundtrip averaged pump (dashed) and signal (solid) intensities. (Upper right) Instantaneous pump intensity. (Lower right) Instantaneous signal intensity. τ denotes the periodicity due to the cavity roundtrips.

For cavity length ratios that are fractions m/n instead of integers the signal will only interact with the same part of the pump period every n passes. In this case the resonant enhancement is reduced as the signal has now also interacted with other, incoherent, parts of the pump. This is in good agreement with our experimental results. When the pump energy is increased the oscillation threshold will be reached also for other parts of the pump pulse and not only at high intensity fluctuations caused by the coherent addition of the pump modes. This temporally broad signal will reduce the length resonance contrast. Back-conversion will also reduce the pump-signal cross-correlation.

The cavity length resonances can of course also be explained in the frequency domain, and this may give some additional insight into the phenomenon. Equal cavity lengths of pump laser and OPO will mean that the longitudinal mode separation in the pump and the signal is the same. Let us study a single idler frequency, generated by difference frequency generation (DFG) between one longitudinal mode in the pump and one longitudinal mode in the signal. This idler frequency will through DFG with other pump modes generate radiation at other OPO cavity modes that becomes longitudinal modes in the signal. This cross-seeding of the signal modes will transfer the phase relationship between the pump modes to the signal modes, and generate the cross-correlation between signal and pump that is seen in the time domain. If the mode separation of the pump and the signal do not match, the seed that is generated by DFG between pump modes and an idler frequency will not match any OPO cavity mode. The signal modes will then start oscillating independently and experience lower gain than in the length matched cavity.

Correlation between pump modes, as in a partially mode-locked laser, will increase the height and contrast of the intensity spikes in the pump. This will increase the amplitude of cavity length resonances and make them persist higher above threshold. For a perfectly mode-locked laser we would have the well known length matching requirement for a synchronously pumped OPO [5,6].

#126746 - $15.00 USD Received 13 Apr 2010; revised 5 May 2010; accepted 5 May 2010; published 7 May 2010

The presence of the dips surrounding the length resonances in a SRO might be an additional indication that the SRO resonances are in fact the result of time-periodic coherent addition to the signal field for consecutive passes in the SRO cavity. Considering that the pump and the SRO signal mode spectra are fixed by the respective cavities, a small change in the SRO cavity length will result in the situation where a number of pump Fabry-Perot modes will correspond to the minima of the signal Fabry-Perot modes, i.e. these pump modes for the consecutive passes will interact with signal field phase-shifted by $\pi/2$. This will result in periodic and coherent deamplification of the parts of the signal field, producing dips in the output energy. This effect is not observed in a broadband DRO, as seen in Fig. 3, because the signal and idler spectra in the DRO will change in response to the cavity length variation, for instance by starting to oscillate on other mode clusters where the gain is stronger. The narrow spectral extent imposed by the VBG output coupler in the SRO should be expected to be an important factor in giving rise to the dips in the SRO efficiency as the total conversion efficiency is a result of coherent and incoherent summation over an ensemble of signal modes. For a broadband SRO pumped by partially coherent Q-switched pulses, the longitudinal mode distance variation due to group delay dispersion can be expected to decrease the amplitude of SRO length resonances and antiresonances (dips). In principle the proposed model explains both the resonant and antiresonant SRO behavior but we cannot rule out some additional effects producing dips in the SRO efficiency for certain cavity lengths. More detailed understanding would need further investigation.

In conclusion we have shown that the phenomenon of enhanced OPO efficiency for a fractional ratio between the OPO and the pump laser cavity optical path lengths is present for both singly and doubly resonant cavities. In the SRO the resonance enhancement becomes possible when there is a cross-correlation between pump and signal after one roundtrip in the OPO cavity. The mechanism is most efficient close to threshold where the OPO only reaches threshold for the periodic intensity spikes of the multimode pump laser. The efficiency of the enhancement mechanism also depends on the mutual coherence of the longitudinal modes of the pump. In the case of total coherence, as in mode-locked lasers, the SRO output enhancement mechanism should be analogous to synchronous pumping employed in picosecond and femtosecond SROs.

Acknowledgements

We acknowledge valuable discussion with Darrel Armstrong, Sandia National Labs, USA, and Gunnar Arisholm, FFI, Norway. We also acknowledge FFI, Norway, for providing us with the OPO modeling tool Sisyfos. The Swedish Research Council provided partial funding for this work.

#126746 - $15.00 USD Received 13 Apr 2010; revised 5 May 2010; accepted 5 May 2010; published 7 May 2010